AUTOFOCUS IN MULTISTATIC PASSIVE SAR IMAGING

Kuang-Hung Liu and David C. Munson, Jr.

Department of Electrical Engineering and Computer Science
University of Michigan, Ann Arbor, MI, 48109

ABSTRACT

Synthetic Aperture Radar (SAR) imaging suffers from image focus degradation in the presence of phase errors in the received signals due to unknown platform or target motion. We study automatic focusing (autofocus) under a multistatic passive scenario, where the illumination is provided by a set of stationary UHF transmitters and the goal is to image a moving aircraft. We employ heuristic iterative estimation algorithms that maximize a sharpness metric of the image. A similar method has been studied for the case of mono-static radar, where only one antenna is used for both transmitting and receiving. We present simulation results to help assess the effectiveness of the proposed autofocus approach.

***Index Terms*—** SAR, autofocus, sharpness, phase estimation

1. INTRODUCTION

Passive multistatic Synthetic Aperture Radar *(SAR)* has been studied for imaging aircraft using reflected TV or FM radio signals [1]. We assume there are multiple transmitters located at different locations and possibly multiple receivers, also not collocated. As the aircraft traverses its flight path, the receivers collect samples of the radio signals reflected from the target. We further assume there is a target tracking system that will provide us an approximate location of the aircraft associated with each instant in time.

The relationship between the aircraft image and the collected returned signal can be conveniently explained using a tomographic formulation of SAR [2][3], which allows us to view returned signals as data lying in the *Fourier domain* of the target reflectivity. Each narrow-band transmitter provides data on one arc in Fourier space. Multiple transmitters give data on multiple arcs. By first interpolating the data on these multiple arcs to a Cartesian grid, we can use an FFT to form the final aircraft image.

Because the target tracking system will give us only an estimated location of the aircraft, the associated timing errors in the demodulation will cause the reconstructed image to suffer distortion. One way to remedy this undesired effect is to apply autofocus techniques to the image formation process [4]. Much of the work in autofocus for SAR imaging has been for the case of monostatic SAR. Although the concepts behind image formation for different kinds of SAR systems (monostatic, bistatic, multistatic) are similar, several key assumptions that are crucial in the development of autofocus algorithm for monostatic SAR fail to apply to the bistatic and multistatic cases. Thus, it is inappropriate to apply existing autofocus algorithms to bistatic and multistatic SAR [4].

We introduce the imaging model and establish notation in Section 2. In Section 3, we introduce one possible autofocus algorithm that is motivated by the *Stage by Stage Approaching (SSA)* autofocus algorithm [5]. This algorithm can be further simplified if we add an assumption regarding the smoothness of the aircraft flight path, as discussed in Section 4. Simulation results are presented in Section 5.

2. IMAGE MODEL

The geometry of the system is shown in Fig.1. We take the

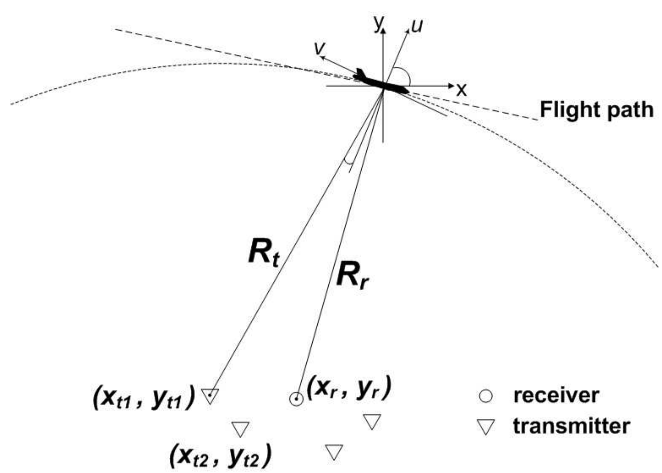

Fig. 1. Geometry of the multistatic SAR system.

altitude of the aircraft to be zero for simplicity, and we make the far-field assumption. The transmitter transmits a narrow-band signal that is nearly sinusoidal, i.e. the real part of

$$s(t) = exp\{j(\omega_o t)\} \ .$$

1-4244-1484-9/08/$25.00 ©2008 IEEE

The collected return signal is then demodulated with in-phase and quadrature versions of the transmitted signal, $Re(s(t))$ and $-Im(s(t))$, each delayed by $(R_t + R_r)/c$, where R_t and R_r are the distances of the transmitter and receiver to the target. R_t and R_r are estimated by the target tracking system. The estimated values of R_t and R_r are denoted as $\tilde{R}_t$ and $\tilde{R}_r$. The estimation error causes a time delay error of $\varepsilon = ((R_t + R_r) - (\tilde{R}_t + \tilde{R}_r))/c$ in the demodulation process. After demodulation, the collected data resides on multiple arcs in Fourier space. Demodulation errors caused by imprecise knowledge of the round-trip distance from transmitter-to-target-to-receiver induce a phase error in the collected Fourier data. This phase error can be compensated once we have an accurate estimate of R_t and R_r.

Let $m = 0, \ldots, M-1$ be the indices for the discrete locations of the aircraft, at uniformly spaced points in time, as it traverses the flight path. We call the return signals collected for the sample time m the data for *range bin m*.

3. AUTOFOCUS BASED ON SSA APPROACH

One possible autofocus algorithm for multistatic SAR imaging is motivated by the SSA algorithm [5], which iteratively compensates phase error for each range bin independently. The compensating phase error estimate is obtained by an optimization algorithm that tries to maximize a particular image sharpness measure. The sharpness measure is defined as

$$C(g) = -\sum_{m=0}^{M-1}\sum_{n=0}^{N-1} I_{mn}\ln(I_{mn})$$

where

$$I_{mn} = \frac{|g(m,n)|^2}{\sum_{k=0}^{M-1}\sum_{l=0}^{N-1}|g(k,l)|^2}$$

and $g(m,n)$ is the imaged target [6]. The data collected by each transmitter-receiver pair for a particular sample point m will suffer different phase errors due to the different locations of the transmitters. However, the errors at a given time are all caused by the same misestimation of the target position. And we can infer the phase error for each of the transmitter-receiver pairs by estimating the true location of the aircraft. Here, instead of searching for the optimal phase solution as in the SSA approach, we try to find the target position that will best compensate the phase error. We accomplish this by doing a 3 by 3 grid search with the current estimated location as the center. The new estimate is the location that gives the maximum image sharpness. We proceed in an iterative fashion, halving the size of the grid at each stage. The algorithm process is described as follows.

NOTATION

1. *stage* denotes the current stage of the algorithm.
2. *stepsize* controls the position increment in the current stage.
3. λ_n is the wavelength corresponding to the frequency of the n*th* transmitter.
4. $location_m(x,y), 0 \le m \le M-1$ is the estimated target position needed to compensate the phase error; this is updated as the algorithm proceeds.
5. $Threshold$ is used to terminate the inner loop of the algorithm.

step 1: Initialization, set *stage* = 0, *stepsize* = $\max_n(\lambda_n)$, $0 \le n \le N-1, location_m = (0,0), 0 \le m \le M-1$.

step 2: Estimate the position of the target in the current stage. Do this range bin by range bin.

(a) For sample point m (range bin m), use the 3 by 3 search grid with $searchlength = stepsize$. There are nine candidate positions (x_1, y_1),..., (x_9, y_9); we calculate the compensating phases $\varphi_i(1)$,...,$\varphi_i(N-1)$ that will apply to the collected Fourier data if we shift the current position to the new position (x_i, y_i) $i = 1, \ldots, 9$. Compensated Fourier data is

$$\hat{F}_i(m,n) = F(m,n)e^{j\varphi_i(n)}, i = 1, \ldots, 9 \ .$$

Interpolate the polar-formatted data $\hat{F}_i$ to the Cartesian grid $\hat{G}_i$, and then we calculate the corresponding image sharpness metric for $\hat{g}_i$ (where $\hat{g}_i = DFT^{-1}\{\hat{G}_i\}$). Select the estimated position that gives the minimum value of the sharpness metric:

$$optimal_m(x,y) = \arg\min_{i=1,\ldots,9}(C(\hat{g}_i)) \ .$$

The metric based on this optimal estimated position is

$$C_{optimal_m}(\hat{g}) \ .$$

Repeat the same process for m from 0 to $M-1$.

(b) Compute the relative change of the metric between the current and previous iteration, that is, calculate

$$\Delta C = \left|\frac{C_{location_m}(\hat{g}) - C_{optimal_m}(\hat{g})}{C_{location_m}(\hat{g})}\right| \ .$$

If $\Delta C > Threshold$, which means that there is an obvious change in the image sharpness, then go back to **step 2**, or else go to **step 3**. In either case update $location_m$ with $optimal_m$.

step 3: Update the stage:

$$stage = stage + 1 \ .$$

Update the position increment:

$$stepsize = stepsize/2 \ .$$

If $stage > 6$, we terminate the algorithm process, or else go back to **step 2**.

We terminate the algorithm when $stage > 6$ which corresponds to a phase error less than 6 degrees.

4. AUTOFOCUS BASED ON SMOOTH FLIGHT PATH ASSUMPTION

In the previous section we considered an approach that is suitable for the worst case of phase error, which is *i.i.d* for each of the data sample points. When imaging using long wavelengths (e.g. FM, television band) the flight path will be smooth on the scale of a wavelength. And considering the limited maneuverability of even modern aircraft, it is reasonable to assume that the motion of the aircraft will not behave randomly across our observed flight path. We suggest that the trajectory of the aircraft be modeled by a polynomial function, where the order of the polynomial depends on the maneuverability of the aircraft. Then we only have to estimate the coefficients of the polynomial, which reduces our number of unknowns drastically.

The algorithm begins with an initial estimate of the flight trajectory obtained by the target tracking system, which is also assumed to be smooth. Although this estimated flight path will not match the true path, it will allow us to determine the order of the polynomial that is required to describe the true flight path. Here we take the altitude to be zero for simplicity, we use two polynomials to describe the X and Y flight coordinates as a function of time. The algorithm is described as follows.

step 1: Initialization, set *stage* = 0, *stepsize* = $\max(\lambda_n)$, obtain flight path location (x_i, y_i) $i = 1, \ldots, M$ from the target tracking system.

step 2: Estimate the order of the polynomial that is needed to accurately describe the flight path. Let the two polynomials that describe the X and Y coordinates be

$$p_x(t) = \sum_{i=1}^{n} \alpha_i t^i \ , \quad p_y(t) = \sum_{i=1}^{m} \beta_i t^i$$

where n and m are the orders for $p_x(t)$ and $p_y(t)$, chosen to satisfy

$$|x_i - p_x(t_i)| < \epsilon \ and \ |y_i - p_y(t_i)| < \epsilon \ \ i = 1, \ldots, M \ .$$

The α_i and β_i are the coefficients for the polynomials and are found by using least squares estimation.

step 3: Instead of estimating the location of each of the sample points as in Section 3, we now adjust the coefficients of the polynomial (either p_x or p_y) one at a time to maximize the sharpness of the corresponding image according to the sharpness measure $C(g)$ defined in Section 3. Each time we adjust the coefficient, we choose the new coefficient value so that the maximum deviation of the corresponding polynomial is equal to *stepsize*.

step 4: Update *stage* and *stepsize* as in **step 3** in Section 3. If $stage > 6$, terminate the algorithm process, or else go back to **step 3**.

5. SIMULATION RESULTS

In this section, we present simulation results using the two proposed algorithms. The assumed multistatic SAR geometry is shown in Fig 2.(a). The scenario comprises 14 transmitters in the UHF band and two receivers with the parameters listed in Table 1. Fig 2.(b) shows the Fourier grid on which data is acquired by the transmitter-receiver geometry, flight path, and frequencies specified in Fig 2.(a) and Table 1. We used a simulated aircraft image. Although we consider only a 2-D geometry, the extension to 3-D is straightforward. In a true 3-D scenario, we would image the aircraft from below, in which case we could see both sides of the aircraft. The actual flight path corresponds to a smooth s-turn with acceleration and deceleration. The target tracking system reports a smooth s-turn flight path, but deviates from the true path by more than a wavelength. The reconstructed image with and without location estimation error is shown in Fig 2.(c) and (d). The restored image using the two proposed algorithms is shown in Fig 2.(e) and (f). Both algorithms are capable of restoring the image. Because the autofocus algorithm using the smoothness constraint has fewer unknown parameters to estimate, it requires much less execution time than the autofocus algorithm based on the SSA approach. The execution time for the algorithm based on the smooth flight path assumption was only 5% of the time required by the algorithm based on SSA. The order of polynomial needed to describe this particular flight path example was 2 for the X coordinate and 10 for the Y coordinate.

Table 1. Simulation parameters

Antenna parameter			
Frequency (MHz)	Location (x,y)	Frequency (MHz)	Location (x,y)
638	(20,-20)	560	(10,-3)
566	(-10,-3)	572	(-3,-10)
578	(0,-10)	584	(5,-8)
590	(-5,-8)	596	(7,-8)
602	(-7,-8)	608	(8,5)
614	(-8,-5)	620	(10,-5)
626	(-6,-5)	632	(-20,-20)

6. CONCLUSION

In this work, we have studied two metric-based autofocus algorithms for passive multistatic SAR. The autofocus method based on SSA works for all types of estimation error. A smooth flight path assumption allows us to model the flight path using polynomials, thereby reducing the number of unknowns and providing a more efficient algorithm.

7. REFERENCES

[1] Yong Wu and Jr. David C. Munson, “Multistatic synthetic aperture imaging of aircraft using reflected television signals,” *Proc. of SPIE, Algorithms for synthetic aperture radar imagery VIII*, vol. 4382, 2001.

[2] Orhan Arikan and Jr. David C. Munson, “A tomographic formulation of bistatic synthetic aperture radar,” *Intern. Conf. on Advances in Communicartion and Control Systems*, pp. 289–302, 1988 Baton Rouge, La.,.

[3] Jr. David C. Munson, James Dennis O’Brien, and W. Kenneth Jenkins, “A tomographic formulation of spotlight-mode synthetic aperture radar,” *Proc. IEEE*, pp. 917–925, 1983.

[4] Jr. Charles V. Jakowatz, Daniel E. Wahl, Paul H. Eichel, Dennnis C. Ghiglia, and Paul A. Thompson, *Spotlight-Mode Synthetic Aperture Radar: A Signal Processing Approach*, Kluwer Academic Publishers, 1996.

[5] Li Xi and and Jinliu Ni Liu Guosui, “Autofocusing of isar images based on entropy minimization,” *IEEE Transactions on Aerospace and Electronic Systems*, vol. 35, pp. 1240–1252, Oct 1999.

[6] J. R. Fienup and J. J. Miller, “Aberration correction by maximizing generalized sharpness metrics,” *Optical Society of America*, vol. 20, no. 4, pp. 609–620, 2003.

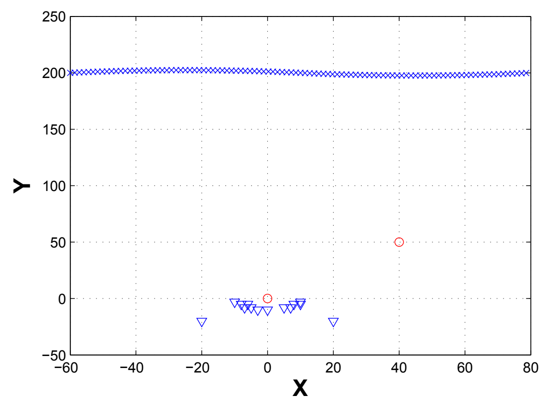

(a) Geometry of the multi-static SAR(◯ : receiver location, ▽ : transmitter location, X : actual flight path).

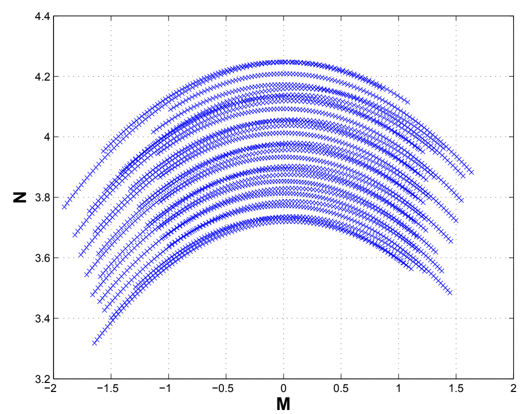

(b) Fourier data collected by multistatic SAR.

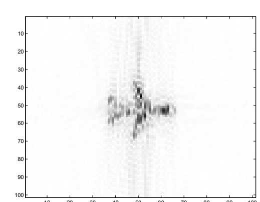

(c) Image without location estimation error.

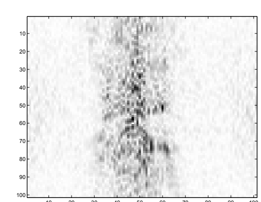

(d) Image with location estimation error.

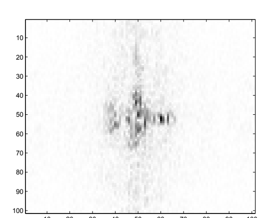

(e) Image reconstructed by using SSA-like autofocus algorithm.

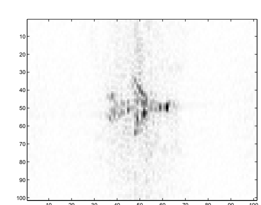

(f) Image reconstructed by using autofocus algorithm based on smooth flight path assumption.

Fig. 2. Experimental results.